SUPPLEMENTARY MATERIAL

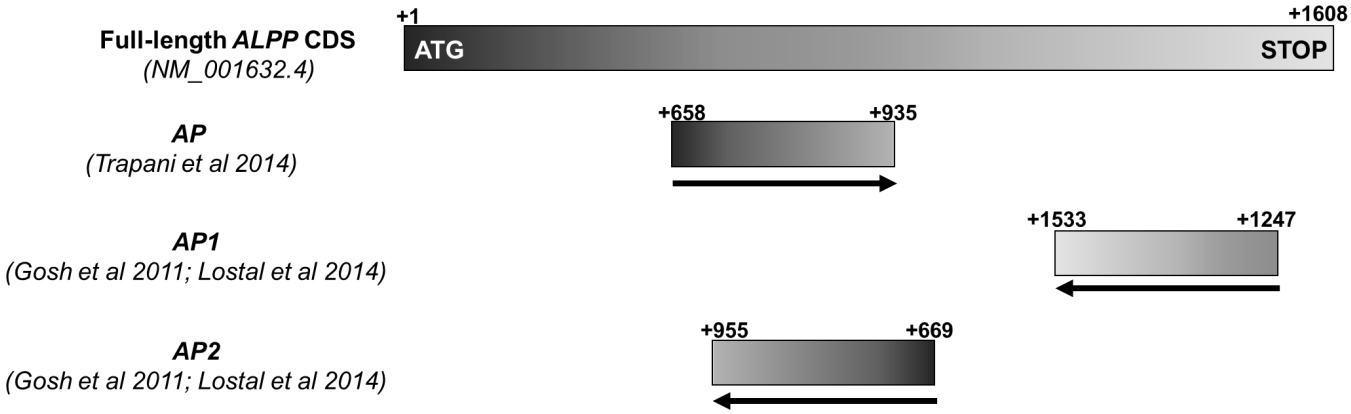

Supplementary Figure S1. Schematic representation of the AP, AP1 and AP2 regions of homology derived from ALPP (placental alkaline phosphatase) used in this study.
CDS: coding sequence

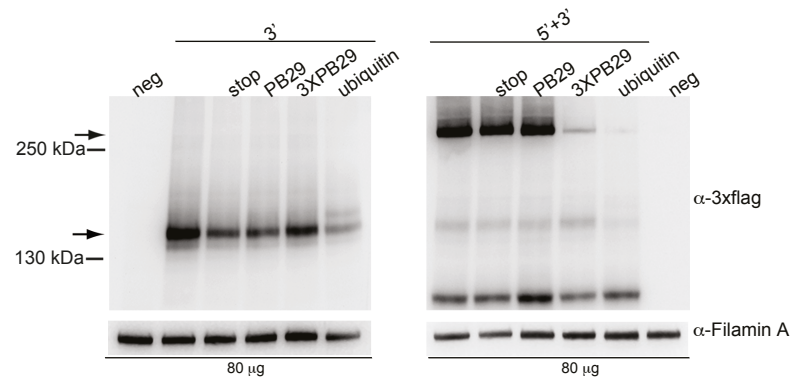

Supplementary Figure S2. Inclusion of degradation signals in the 3'-half vectors does not result in significant reduction of truncated proteins. Representative Western blot analysis of HEK293 cells infected with dual AAV2/2 hybrid ABCA4 vectors containing different degradation signals. The upper arrow indicates the full-length ABCA4 protein, the lower arrow indicates truncated protein products; the molecular weight ladder is depicted on the left. The micrograms of proteins loaded are depicted below the image. The Western blot images are representative of n=3 independent experiments. 5'+3': cells co-infected with 5'- and 3'-half vectors without degradation signals; 3': cells infected with 3'-half vectors without degradation signals; 3xstop: cells infected with 3'-half vectors containing stop codons; PB29: cells infected with 3'-half vectors containing the PB29 degradation signal; 3xPB29: cells infected with 3'-half vectors containing 3 tandem copies of the PB29 degradation signal; ubiquitin: cells infected with 3'-half vectors containing the ubiquitin degradation signal; neg: control cells infected with EGFP expressing vectors, as negative controls. α-3xflag: Western blot with anti-3xflag antibodies; α-Filamin A, Western blot with anti-Filamin A antibodies, used as loading control.

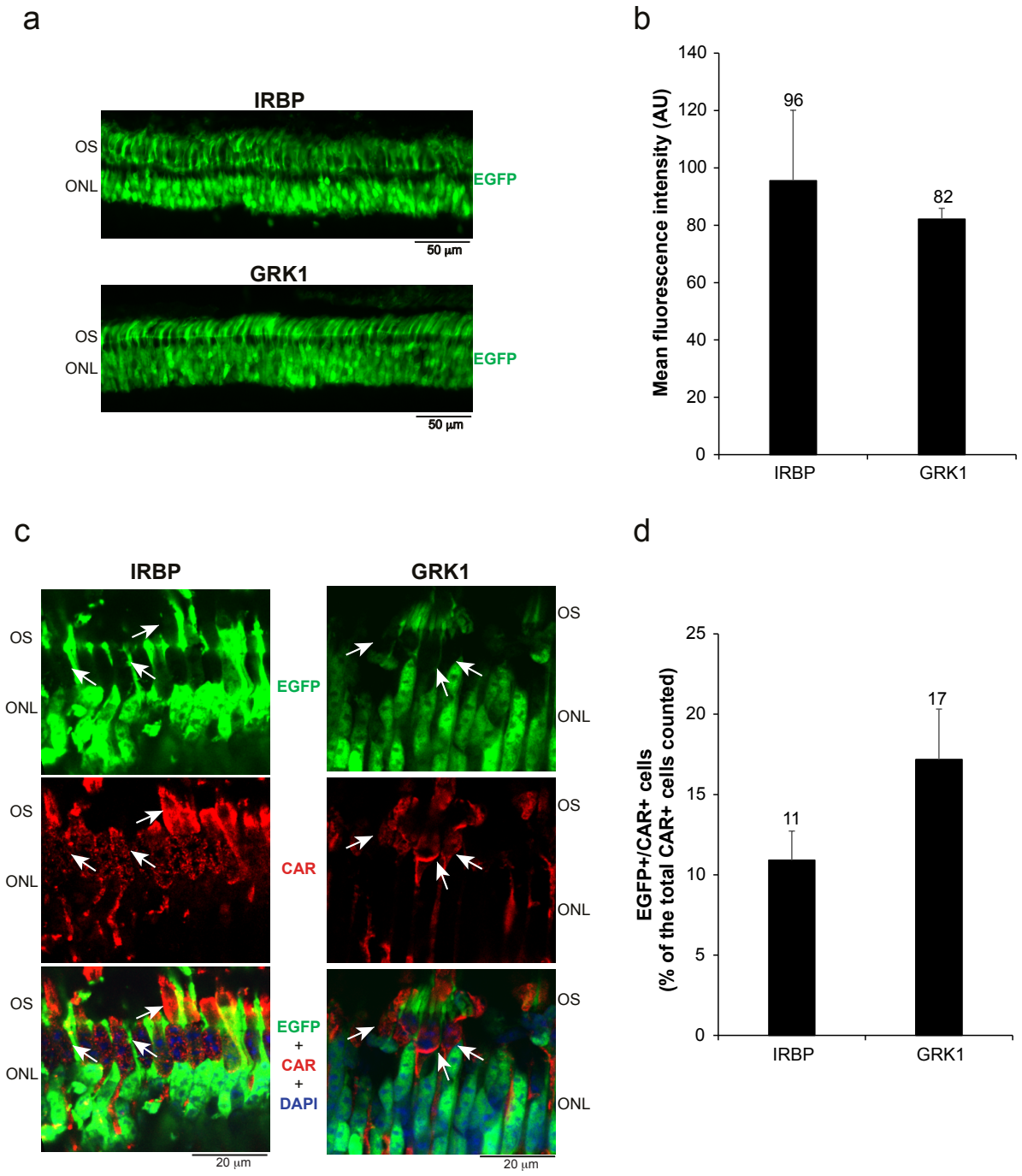

Supplementary Figure S3. EGFP protein expression from the IRBP and GRK1 promoters in pig rod and cone photoreceptors. Three month-old Large White pigs mice were injected subretinally with $1x10^{11}$ GC/eye each of either AAV2/8-IRBP- or AAV2/8-GRK1-*EGFP* vectors. Retinal cryosections were obtained 4 weeks after injection and EGFP was analysed using fluorescence microscopy. (**a-b**) Representative images (**a**) and quantification (**b**) of fluorescence intensity in the PR layer. Fluorescence intensity was quantified for each group of animals on cryosections (six different fields/eye; 20x magnification). (**c-d**) Representative images (**c**) and quantification (**d**) of cone transduction efficiency. Cone transduction efficiency was evaluated on cryosections (six different fields/eye; 63x magnification) immunostained with an anti-LUMIf-hCAR antibody, and is expressed as number of cones expressing EGFP (EGFP+/CAR+) on total number of cones (CAR+) in each field. (**a, c**) The scale bar is depicted in the picture. (**b-d**) n=3 eyes injected with AAV2/8-IRBP-*EGFP* vectors; n=3 eyes injected with AAV2/8-GRK1-*EGFP* vectors**.** Values are represented as mean ± s.e.m. No significant differences were found using Student's t-test. OS: outer segments; ONL: outer nuclear layer; EGFP: native EGFP fluorescence; CAR: anti-cone arrestin staining; DAPI: 4',6'-diamidino-2-phénylindole staining. The arrows point at transduced cones.

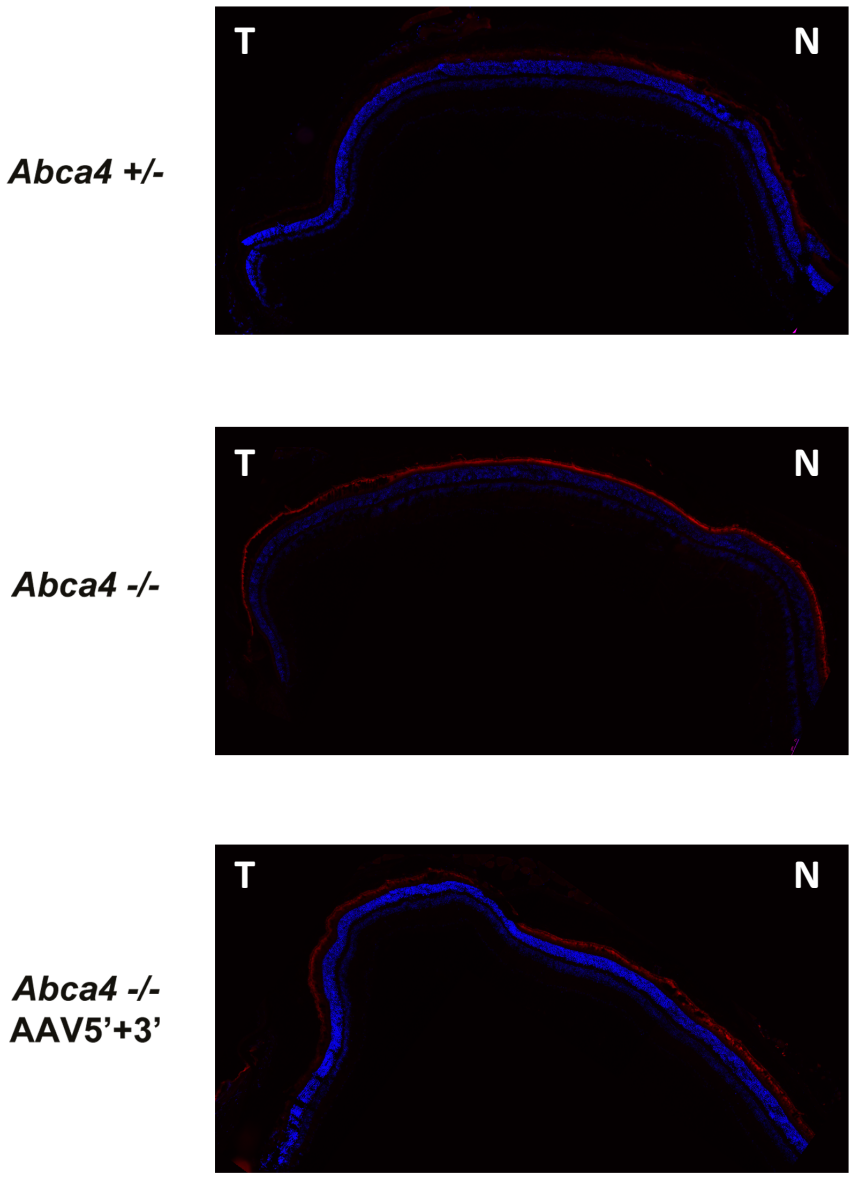

Supplementary Figure S4. Subretinal delivery of improved dual AAV vectors results in significant reduction of lipofuscin accumulation in the Abca4-/- mouse retina. Montage of images of the temporal (injected) side of retinal cross-sections showing lipofuscin autofluorescence (red signal) in the retinas (RPE or RPE+OS) of either pigmented *Abca4+/-* mice not injected or injected with AAV as control (*Abca4+/-*) or pigmented *Abca4-/-* mice either not injected (*Abca4-/-*) or injected with dual AAV hybrid *ABCA4* vectors (*Abca4-/-* AAV5'+3'). n= 4 eyes for each group. T: temporal side; N: nasal side**.**

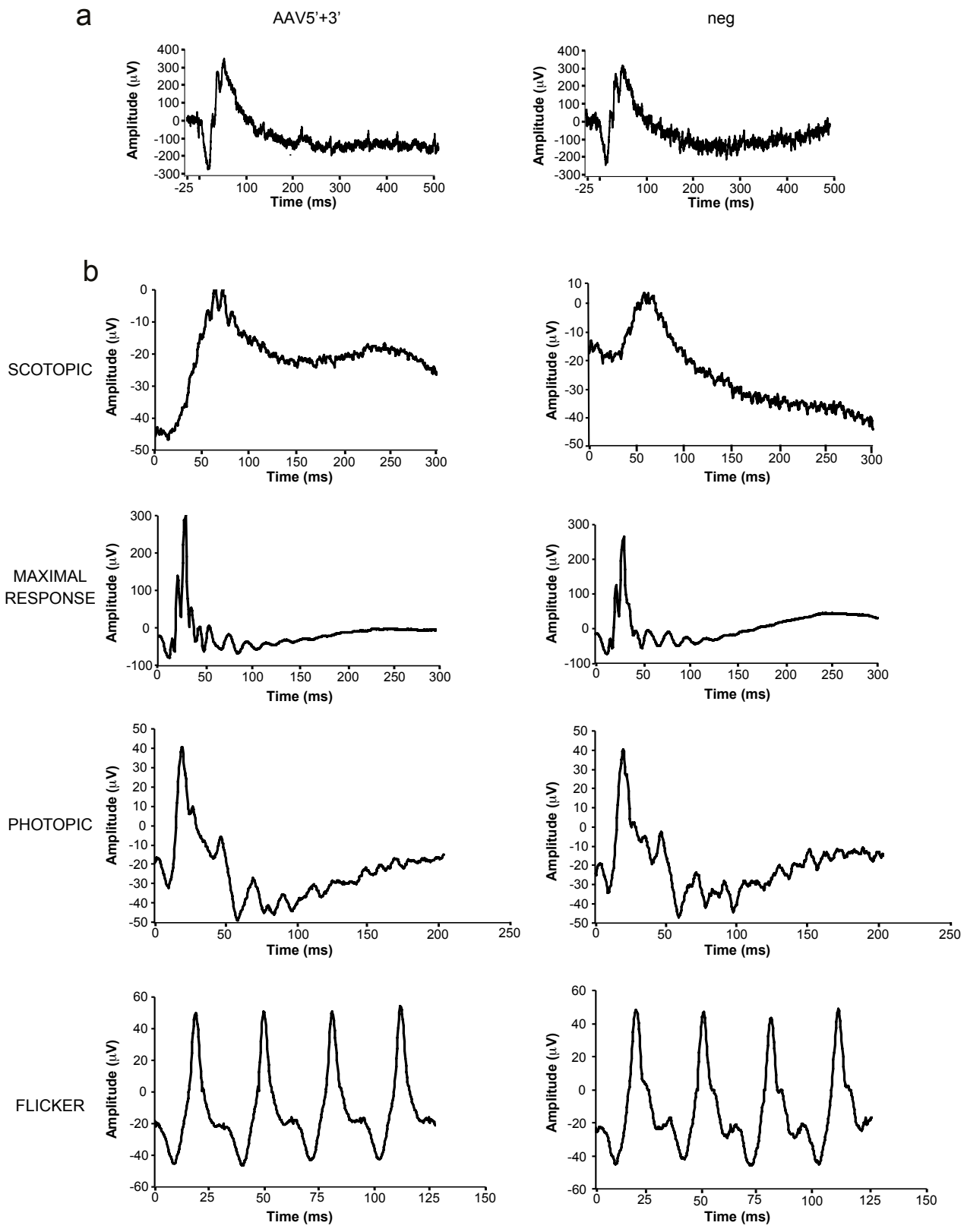

Supplementary Figure S5. Similar electrical activity between either negative control or improved dual AAV-treated eyes in mice and pigs.

Representative ERG traces from C57BL/6 mice one month post-injection of either dual AAV hybrid *ABCA4* vectors (AAV5'+3') or negative controls (i.e. negative control AAV vectors or PBS; neg). (b) Representative traces from scotopic, maximal response, photopic and flicker ERG tests in pigs one month post-injection of either dual AAV hybrid *ABCA4* vectors (AAV5'+3') or PBS.

Supplementary Table S1. Yields of AAV5:2/2 vectors in the presence of various ratios of Rep5 and Rep2 packaging constructs

REP5/REP2	ITR2 TITRE (GC/ml)
1:1	9,0E+10
1:3	2,2E+11
1:10	3,4E+12

GC: genome copies.

Supplementary Table S2. Quantification of full-length ABCA4 relative to truncated protein expression from Western blot analysis of HEK293 cells infected with dual AAV hybrid vectors including miR target sites in the 5'-half vector.

miR TARGET SITES	**FULL-LENGTH ABCA4 / TRUNCATED PROTEIN**	
	+SCRAMBLE	**+miR**
5'-miR-let7b + 3'	1,2 ± 0,3	0,8 ± 0,3
5'-miR-204+124 + 3'	1,8 ± 0,5	2,7 ± 0,9
5'-miR-26a + 3'	1,9 ± 0,8	2,5 ± 1,1

N.B.: Values represent mean ± s.e.m. of the ratios (from three independent experiments) between the intensity of full-length ABCA4 and truncated protein bands in the presence of either the corresponding mimic or a scramble mimic. Ratios in the presence of either the scramble or the corresponding mimic for each pair of vectors were compared using Student's t-test and no significant differences were found.

Supplementary Table S3. Quantification of full-length ABCA4 and truncated protein expression from Western blot analysis of HEK293 cells infected with dual AAV hybrid vectors including degradation signals in the 3'-half vector.

DEGRADATION SIGNALS	FULL-LENGTH ABCA4 / TRUNCATED PROTEIN	
	5'+3' NO DEGRADATION SIGNAL	5'+3' + DEGRADATION SIGNAL
3xSTOP	5,9 ± 1,8	4,9 ± 1,1
PB29		5,3 ± 1,1
3xPB29		1 ± 0,3
ubiquitin		0,6 ± 0,2

N.B.: Values represent mean ± s.e.m. of the ratios (from three independent experiments) between the intensity of the full-length ABCA4 and truncated protein bands from vectors either with or without the degradation signals. More details on the statistical analysis including specific statistical values can be found in the Statistical analysis paragraph of the Materials and Methods section